Bone. Author manuscript; available in PMC: 2021 Feb 1.
Published in final edited form as: Bone. 2019 Nov 12;131:115152. doi: 10.1016/j.bone.2019.115152

Multiscale effects of spaceflight on murine tendon and bone

Alix C Deymier [a,*], Andrea G Schwartz [b], Chanteak Lim [b], Brian Wingender [a], Akhilesh Kotiya [b], Hua Shen [b], Matthew J Silva [b], Stavros Thomopoulos [c,d,*]

Author information Article notes Copyright and License information

PMCID: PMC7138367 NIHMSID: NIHMS1544144 PMID: 31730829

Abstract

Despite a wealth of data on the effects of spaceflight on tendons and bones, little is known about its effects on the interfacial tissue between these two structures, the enthesis. Mice were sent to space on three separate missions: STS-131, STS-135, and Bion-M1 to determine how spaceflight affects the composition, structure, mechanics, and gene expression of the humerus-supraspinatus and calcaneus-Achilles entheses. At the nanoscale, spaceflight resulted in decreased carbonate levels in the bone, likely due to increased remodeling, as suggested by increased expression of genes related to osteoclastogenesis (*CatK*, *Tnfsf11)* and mature osteoblasts (*Col1*, *Osc)*. Tendons showed a shift in collagen fibril size towards smaller diameters that may have resulted from increased expression of genes related to collagen degradation (*Mmp3, Mmp13)*. These nanoscale changes did not result in micro- and milliscale changes to the structure and mechanics of the enthesis. There were no changes in bone volume, trabecular structure, failure load, or stiffness with spaceflight. This lack of tissue-level change may be anatomy based, as extremities may be less sensitive to

spaceflight than central locations such as vertebrae, yet results highlight that the tendon enthesis may be robust against negative effects of spaceflight.

Keywords: enthesis, spaceflight, composition, structure, mechanics

1. Introduction

With increased interest in long-term space exploration, such as the proposed mission to Mars, it has become increasingly important to explore the effects of the space environment on the musculoskeletal system. In particular, decreased loading due to microgravity can cause significant loss of bone and muscle mass and predispose those tissues to injury (1, 2). The effects of disuse on the musculoskeletal system have been examined via a number of earthbound analogues. These model systems have shown that disuse leads to decreased muscle mass, decreased tendon thickness, bone loss, and compromised strength and stiffness of both tendon and bone (3, 4). However, these earthbound analogues are not able to fully capture the effects of spaceflight on the musculoskeletal system (5). Thus, it remains necessary to directly examine how the musculoskeletal system responds to the space environment.

In the last several decades, space-based studies have brought us a wealth of information about how the musculoskeletal system reacts to spaceflight conditions. Much like with the earthbound analogues, decreases in bone and tendon mass as well as compromised mechanics have been reported (3, 6). However, although structural and mechanical changes of individual tissues have been well examined, there is little information about what happens at the interfaces between these tissues. The tendon-to-bone attachment (the “enthesis”) enables the transfer of load from muscles to the skeleton, allowing for joint motion. However, due to the presence of stress concentrators that arise at interfaces between dissimilar materials such as tendon and bone (7–9), the enthesis is at high risk for rupture (10). Furthermore, this interface is particularly sensitive to changes in its loading environment; earthbound studies have shown that 3 weeks of muscle paralysis leads to defects in murine enthesis structure and mechanics at multiple length scales (11). At the millimeter scale, there was a significant loss of trabecular bone. At the micrometer scale, changes in mineral size and orientation led to defects in energy absorption. At the nanoscale, loss of carbonate in the mineral lattice led to stiffening of the mineral. Together, these structural and compositional changes led to an increased risk and extent of failure at the tendon attachment. In the current study, mice from NASA missions STS-131, STS-135, and Bion-M1 were examined after multiple weeks of spaceflight. Changes to the structural, compositional, and mechanical properties of tendon entheses were examined.

2. Materials and Methods

2.1. Sample preparation

Mice for this study (see Table 1 for details) flew on one of three spaceflight missions: STS-131, STS-135, or Bion-M1. For U.S. National Aeronautics and Space Administration (NASA) STS-131, the space shuttle Discovery launched from Kennedy Space Center (KSC; Cape Canaveral, FL, USA) on April 5, 2010, for a 15-d flight, and landed at KSC on April 20, 2010. For NASA STS-135, the space shuttle Atlantis launched from KSC on July 8, 2011, for a 13-d flight, and landed at KSC on July 21, 2011. For the Russian Academy of Sciences, Institute of Biomedical Problems Bion-M1, the space capsule launched on April 19, 2013, from Baikonur Cosmodrome, Kazakhstan, for a 30-d mission, and landed on May 19, 2013, near Orenburg, Russia. During spaceflight, mice were housed in specialized animal enclosure modules—self-contained habitats that provided continuous living space, food, water, ventilation, and lighting (12, 13). Age- and gender-matched mice were housed on the ground in conditions that were identical to those of spaceflight (FL) mice and were used as ground controls (GCs). FL mice were euthanized 2–14 h after landing. Humerus-supraspinatus (HS) complexes as well as calcaneus-Achilles (CA) complexes from STS and Bion-M1 mice were dissected immediately after being euthanized at KSC and at the Institute of Biomedical Problems (Moscow, Russia), respectively. Experimental procedures for STS mice were approved by the Institutional Animal Care and Use Committee of NASA and conformed to the Guide for the Care and Use of Laboratory Animals (National Institutes of Health, Bethesda, MD, USA). The Bion-M1 animal study was approved by the Institutional Animal Care and Use Committee of Moscow State University, Institute of Mitoengineering, and by the Biomedical Ethics Commission of the Institute of Biomedical Problems and conducted in compliance with the European Convention for the Protection of Vertebrate Animals used for Experimental and Other Scientific Purposes (12). The HS and CA complexes were collected and separated for characterization by: microcomputed tomography (μCT) and mechanical testing, Raman spectroscopy, transmission electron microscopy, or qPCR.

Table 1:

Summary of the mice used in this study.

Mission	Mouse Strain	Mouse age at launch (wk)	Mouse gender	Flight Duration (d)
STS-131	C57BL/6J	16	Female	15
STS-135	C57BL/6	9	Female	13
Bion-M1	C57BL/6N	19–20	Male	30

Open in a new tab

2.2. Bone mineral composition

For Raman spectroscopic analysis of the mineral composition, freshly dissected calcanei were collected from six FL and seven GC mice from STS-131, mounted in Optimal Cutting Temperature (OCT) compound, frozen at −80 °C, and sectioned in the sagittal plane to 20 μm on a cryostat. Thin sections of the tendon-to-bone attachment were deposited on glass slides and maintained frozen until spectra could be obtained. Spectra were collected using a laser Raman microprobe (HoloLab Series 5000 fiberoptically coupled Raman Microscope, Kaiser Optical Systems, Inc.) using techniques described previously (14). A 532 nm laser was focused to a ~1 μm beam spot using an 80 × objective (N.A. = 0.85) and delivering 10 mW of power to the surface of the sample. The scattered light was then collected as 32 4-second acquisitions in a backscatter configuration through the objective lens and transmitted to a 2048-channel CCD detector. Raman spectra were collected within the cortical shell of the calcaneus. Spectra were analyzed as previously described (11, 14, 15). Briefly, spectra were background corrected, and peaks within the spectral range 700–1200 Δcm^{-1} were deconvolved with a mixed Gaussian–Lorentzian peak-fitting algorithm in the GramS42® software package (Galactic, Salem, NH). The ratio of peak intensities between the ν_1 P–O stretching band of carbonated hydroxylapatite (~960 Δcm^{-1}) and the aromatic ring stretching band of phenylalanine residues in collagen (~1003 Δcm^{-1}), Fig. 1A, was calculated to represent the mineral-to-matrix ratio. In addition, the peak height ratio of the carbonate ν_1 stretching band in apatite (~1070 Δcm^{-1}) to the phosphate 960 Δcm^{-1} band was determined at each analysis site as a measure of carbonate concentration.

Figure 1:

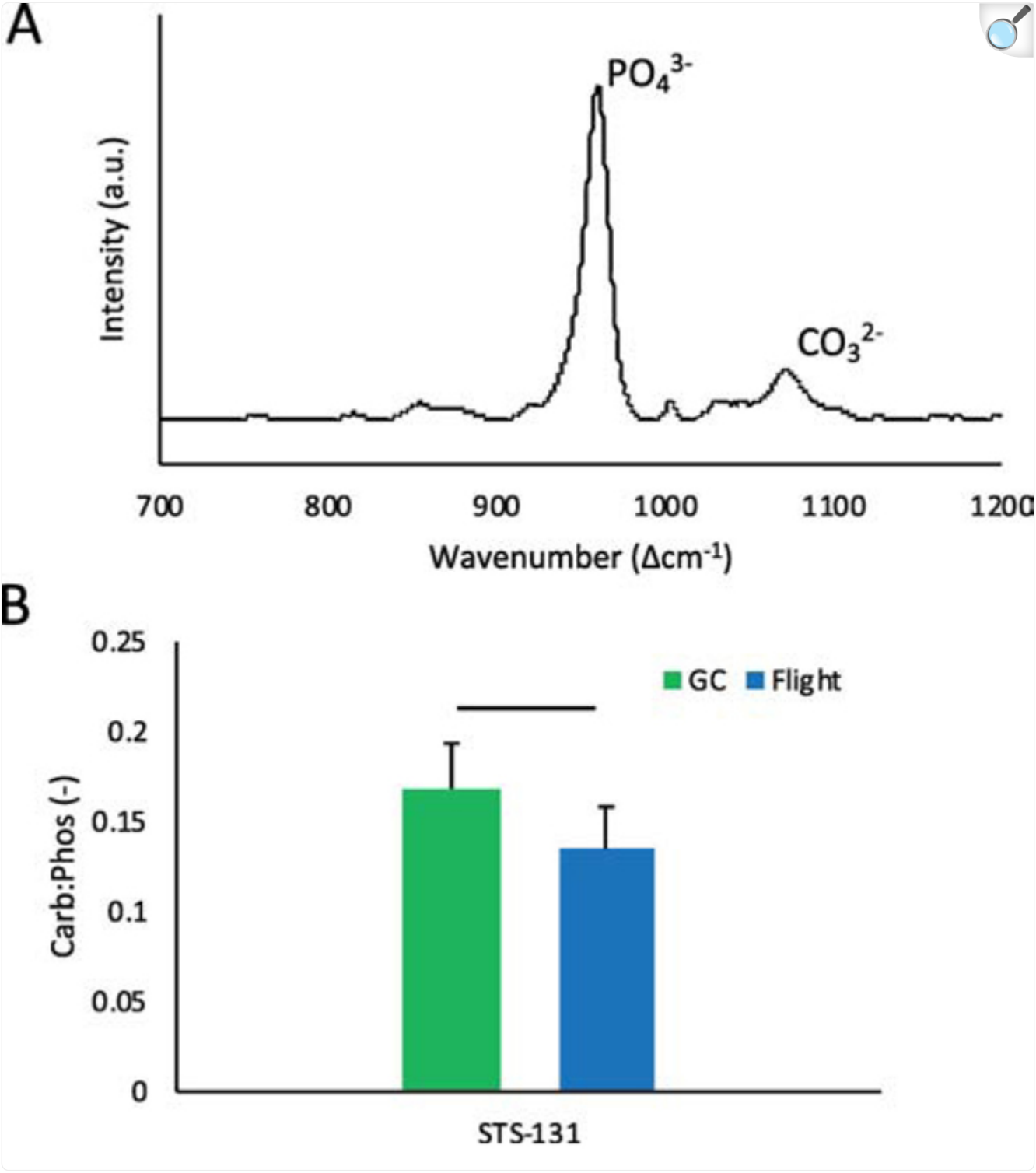

Open in a new tab

(A) Representative Raman trace of calcaneal bone showing the 960 Δcm^{-1} phosphate peak and the 1070 Δcm^{-1} carbonate peak. **(B)** The carbonate-to-phosphate ratio (1070/960) was decreased with space flight in

the calcaneus, indicating loss of carbonate from the bone mineral (GC: ground control; horizontal line above bars: $p<0.05$; STS-131).

2.3. Collagen fibril diameters

Five FL and six GC Achilles tendons from the Bion-M1 mission were frozen immediately after dissection. They were then thawed and fixed in 2% paraformaldehyde, 2.5% glutaraldehyde, and 0.1 M sodium cacodylate, for 1 hr at room temperature. They were washed in 0.1 M cacodylate buffer, and postfixed in 1% osmium tetroxide in cacodylate buffer, pH 7.4 for 1h at room temperature. The tendons were then dehydrated in a graded ethanol series followed by propylene oxide. The tissue was infiltrated with increasing concentrations of Polybed resin mixed with propylene oxide as follows: 1:1 for 4 h, 1:4 for 12 h, final embedding mixture for 8 h. Finally, the tissues were embedded in fresh embedding mixture, and polymerized at 68°C overnight. A microtome was used to section 90 nm thick sections that were deposited on carbon-coated copper grids. The sections were then stained with 2.5% uranyl acetate in EtOH for 30 min at room temperature followed by 30–45 min with 0.2% lead citrate in 0.1 N NaOH. Ultrathin transverse sections were examined in a Hitachi H-7650 TEM operating at 120 kV accelerating voltage. Several brightfield images were taken from each sample with a magnification above 10000X at locations where the fibrils appeared to be oriented perpendicular to the section plane, Fig. 2A. ImageJ software (version 1.51u, NIH) was used to measure the minimum diameter of at least 400 fibrils from each tissue sample. Histograms were generated from this data.

Figure 2:

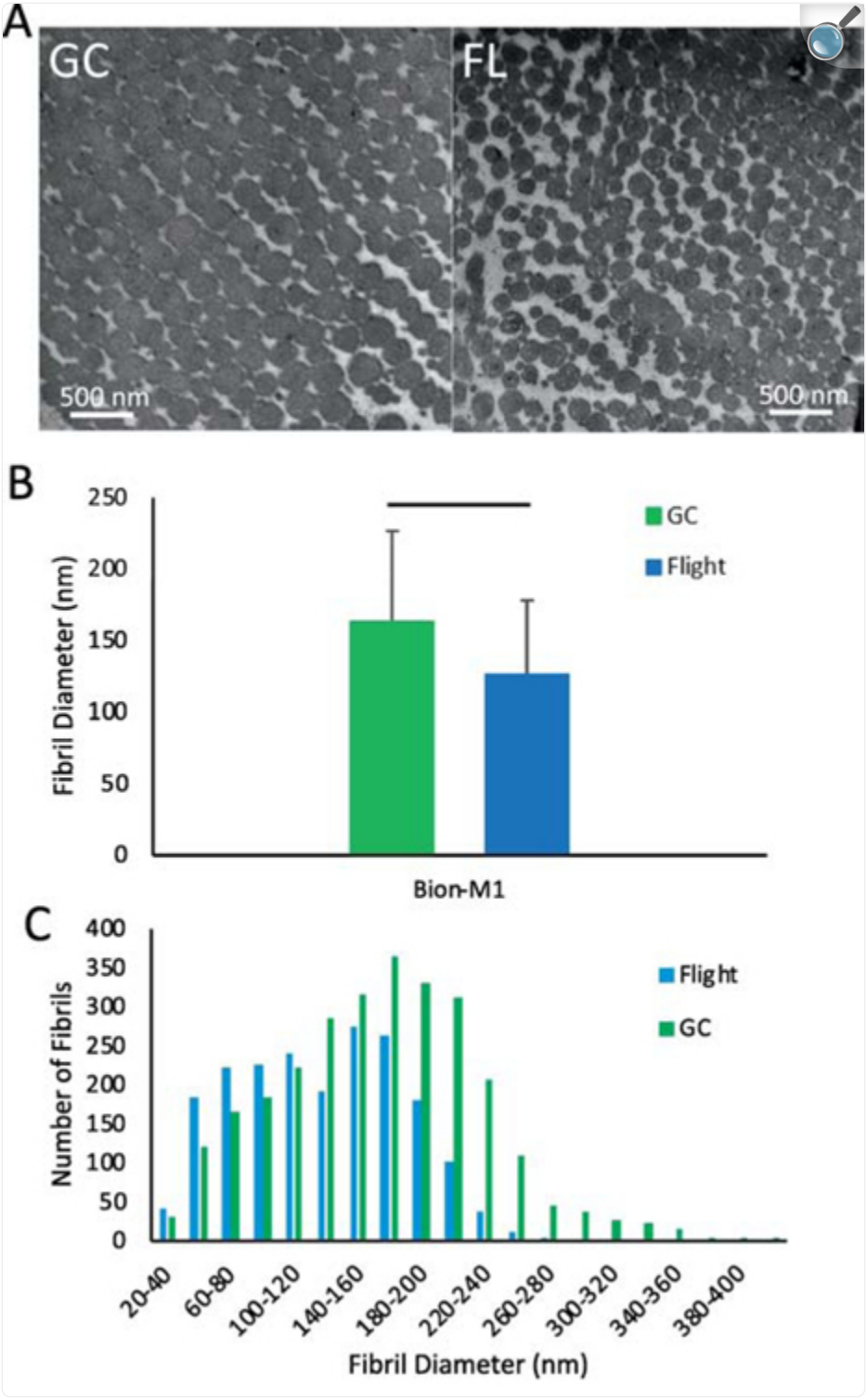

Open in a new tab

(A) Representative TEM images of Achilles tendon cross-sections for ground control (GC) and flight (Bion-M1). **(B)** Spaceflight led to a decrease in the mean fibril diameter of the Achilles tendon (horizontal line

above bars: $p<0.05$). **(C)** The distribution of fibrils shifted towards smaller diameters after 30 days of spaceflight.

2.4. Bone morphometry (μCT)

Six FL and four GC HS samples from STS-131, 13 FL and 13 GC CA samples from STS-135, and 12 FL and 11 GC HS samples from Bion-M1 were prepared and scanned for micro-computed tomography (μCT) analysis. These specimens had been wrapped in gauze soaked in phosphate buffered saline (PBS) and stored at −20 °C prior to analysis. μCT imaging was performed using a Scanco μCT40 scanner (ScancoMedical AG, Switzerland). Scans were performed at X-ray tube settings of 55 kV and 145 μA with a 200 ms integration time at an isometric resolution of 20 μm. The scanned region included the humeral head and the supraspinatus tendon. These scans were used to measure the trabecular morphometry in the humeral head. In the CA samples, cortical thickness in the midsection of the calcaneus, minimum tendon cross-sectional area, and trabecular morphometry in the posterior most 1mm were measured. For the HS, trabecular morphometry was measured in the humeral head above the growth plate.

Bone morphometry values such as the cortical thickness (Ct.Th.), ratio of bone volume/total volume (BV/TV), trabecular thickness (Tb.Th.), trabecular spacing (Tb.Sp.) and trabecular number (Tb.N.) were measured using a built-in software algorithm (Scanco, Zurich, Switzerland). To determine the minimum cross-sectional area of the tendon, cross-sectional areas of sagittal slices through the tendon were determined using thresholding and the minimum cross-sectional area was recorded.

2.5. Mechanical properties

Uniaxial tensile testing was performed to determine the mechanical properties of the entheses of samples from STS-131 (5 FL, 5GC), STS-135 (10 FL, 10 GC) and Bion-M1 (5 FL, 5 GC) as previously described (11, 16) . For the HS complex, after μCT scanning to determine the tendon and enthesis cross-sectional areas, the humerus was potted in epoxy up to the humeral head to stabilize the bone. A paperclip embedded in additional epoxy was placed over the articular surface of the humeral head to minimize the risk of fracture at the growth plate. For the CA complex, a custom loading rig was employed that maintained a 90° angle between the Achilles tendon and the calcaneus to reproduce physiological conditions. Tendons were wrapped in saline-soaked gauze during potting to maintain hydration. Immediately before testing, the tendon was secured between two layers of thin paper with a drop of cyanoacrylate adhesive before being installed in the grips. Samples were tested in a 37°C saline bath attached to an Instron ElectroPuls E1000 (Instron Corp., Canton, MA) fitted with a 5 lb load cell. The tendon gauge length was determined optically. The testing protocol (WaveMatrix software, Instron Corp., Canton, MA) consisted first of a 300 mN for preload for HS and a 150 mN preload for CA followed by 5 cycles of preconditioning consisting of a triangle waveform at 0.1 Hz with a peak

strain of 1%. Tendons were returned to the baseline state for 150 sec for HS and 40 sec for CA before loading to failure at 0.5 %/s for HS and 1%/s for CA.

Estimates of the maximum force and stiffness were made from the load–displacement curves of each load-to-failure test. Material properties were determined by normalizing the force by the minimum cross-sectional area of the tendon as measured via μCT to obtain stresses. Young's modulus and maximum stress were calculated from the stress-strain curves. The linear portion of the curves, used to calculate stiffness and Young's modulus, was identified by adjusting a window of points within the load–deformation or stress–strain curves so as to maximize the R^2 value for a linear least squares regression of the data in the window.

After failure, all HS samples exhibited a failure crater at the tendon-bone attachment site where mineralized tissue was fractured during mechanical testing, Fig. 4H. The area of the crater was measured by reconstructing the 3D volume of the humeral head from the μCT slices in Osirix (Pixmeo, Bernex, Switzerland) and determining the area of the crater via ImageJ (17). In ImageJ, the outline of the crater was drawn by an experienced operator such that it included all areas where mineralized tissue had been removed. The crater area was determined from the area of the drawn shape using the program's built-in area measurement tool.

Figure 4:

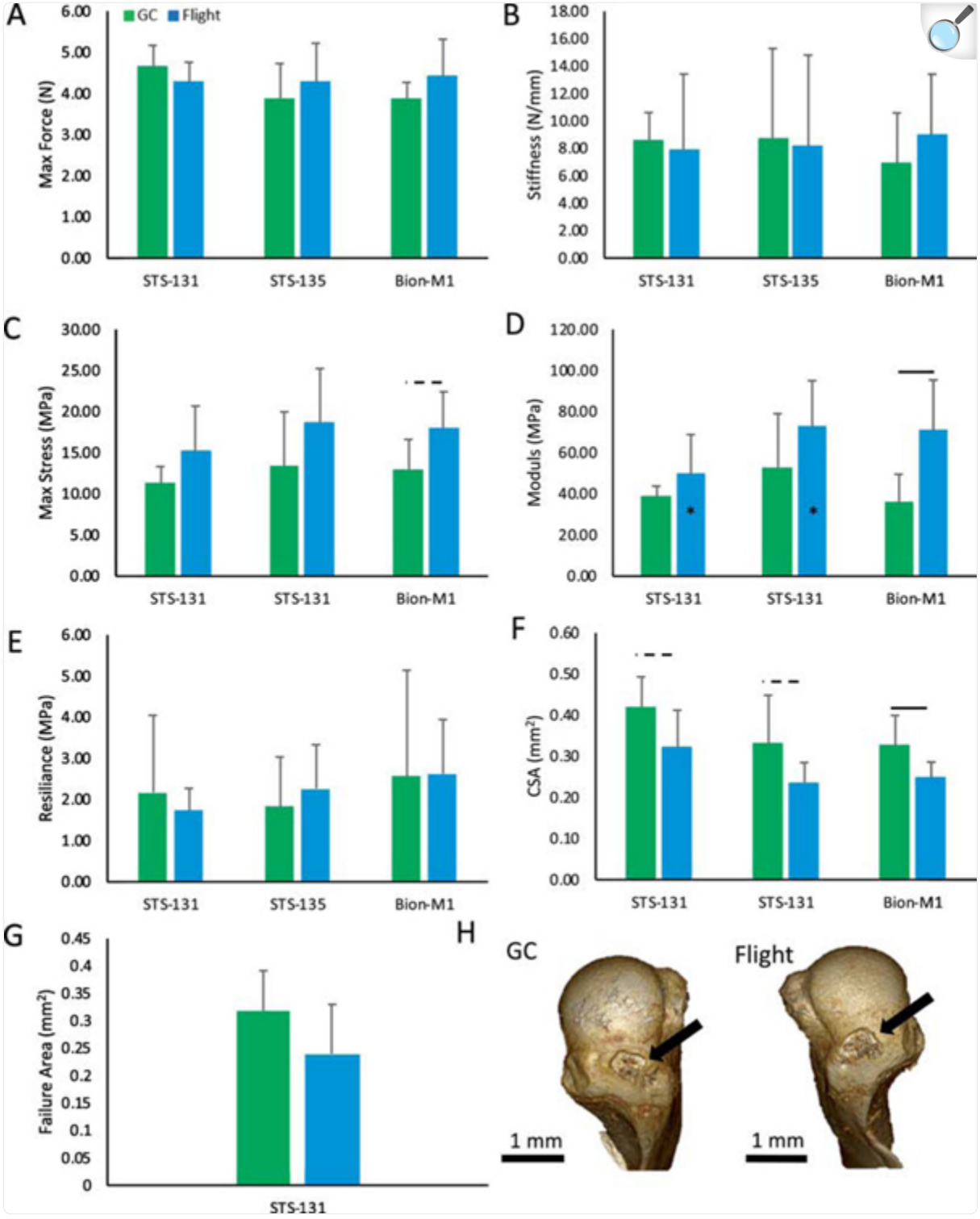

Open in a new tab

Spaceflight had few effects on the mechanics of the supraspinatus tendon enthesis. **(A-B)** The structural properties maximum force and stiffness were not significantly changed by spaceflight. **(C-E)** The material

properties maximum stress, modulus, and resilience were not significantly changed by spaceflight. There was a trend towards increased modulus due to spaceflight for the Bion-M1 mission. **(F)** Cross-sectional area was decreased for all three missions. **(G-H)** All of the samples failed via tendon enthesis avulsion, resulting in a crater at the failure area (arrows in H). The failure area was not significantly different between the GC and flight samples. (Horizontal line above bars: $p<0.05$, dashed line above bars: $p<0.1$) (Significant differences between missions i.e., flight STS-131 vs. flight STS-135, indicated by * within each bar).

2.6. RNA isolation and quantitative RT-PCR

Mouse shoulders were isolated from STS-131 ground control (n=7) and spaceflight (n=7) mice after sacrifice and placed in RNAlater (Qiagen, Valencia, CA, USA) to preserve RNA. The mice on this mission were sacrificed approximately 2–4 hrs after landing. Infraspinatus (IS) and supraspinatus (SS) tendon entheses as well as marrow-free humeral shafts were subsequently dissected, frozen in liquid nitrogen, and pulverized with Mikro-Dismembrator U (B. Braun Biotech International, Melsungen, Germany). For the entheses, total RNA was isolated with the Arcturus PicoPure RNA isolation kit (Applied Biosystems, Forster City, CA) according to the manufacturer's instructions. 400 ng of total RNA were reversely transcribed into cDNA using the SuperScript VILO cDNA Synthesis Kit (Life Technologies). For humeri, total RNA was extracted with Trizol reagent (Ambion) and RNeasy mini kit (Qiagen) as previously described (18). 500 ng of total RNA were reversely transcribed into cDNA as described above. The relative abundances of target genes were determined with a SYBR green-based quantitative real-time PCR using *Gapdh* as the endogenous reference gene. The data are shown as fold changes compared to the gene expression levels of ground control mice ($2^{-\Delta\Delta Ct}$ value). All quantitative RT-PCR primers used in this study were purchased from Qiagen (Hilden, Germany).

2.8. Statistical Analysis

When analyzing the significance of the measured outcomes, it was necessary to account for the effects of the specific mission (STS-131, STS-135, and Bion-M1) from the effects of spaceflight (GC vs. FL). To do this, a 2-way ANOVA was performed for the factors mission and spaceflight. Significance was defined as $p < 0.05$. Post-hoc comparisons were performed using Tukey tests. For the fibril diameter, the Kolmogorov-Smirnov 2-sample test was used to compare the distribution of all diameters measured in the FL group to that in the GC group. All statistical calculations were performed in Minitab18 (Minitab Inc., State College, PA).

3. Results

3.1. Nanoscale: Mineral Composition

Raman analysis of the cortical shell of the calcaneus demonstrated that carbonate levels in the bone mineral were significantly decreased after 15 days of spaceflight (STS-131, Fig. 1). The ratio of the carbonate to phosphate peak height shifted from 0.168 ± 0.025 in the ground control samples to 0.135 ± 0.023 after 15 days of spaceflight (p=0.006). There was no significant change in the mineral-to-matrix ratio with values of 14.1±2.8 and 17.3±6.9 for the GC and FL samples respectively (p=0.31).

3.2. Nanoscale: Fibril Diameter

The distribution of Achilles tendon fibril diameters was significantly affected by spaceflight. The Kolmogorov-Smirnov test confirmed that the two distributions were different (test statistic 0.101> critical value 0.045). After 30 days of spaceflight, there was a distinct shift from larger fibril diameters to smaller fibril diameters in the tendon (Bion-M1, Fig. 2). The average fibril diameter across all samples decreased from 163 ± 63 μm for the ground control samples to 126 ± 51 μm for the tendons exposed to 30 days of spaceflight (p<0.0001). There was no significant change in percent fibril area (71 ± 8% for flight and 72 ± 4% for ground control).

3.3. Microscale: Bone morphometry

Spaceflight did not lead to statistically significant changes in bone morphometry of the humeral head and the calcaneus (Fig. 3). Compared to ground controls, humeral head BV/TV was unchanged due to spaceflight for both the 15-day and 30-day time points (STS-131: p=0.41, Bion-M1: p=0.51; Fig. 3). Similarly, the trabecular structure was unaffected by spaceflight; there were no changes in trabecular thickness (STS-131 p=0.40, Bion-M1: p=0.60), trabecular number (STS-131: p=0.78, Bion-M1: p=0.67), and trabecular spacing (STS-131: p=0.66, Bion-M1: p=0.74) in the spaceflight samples compared to ground control samples (Fig. 3). Although BV/TV did not differ between missions, Tb.Th. and Tb.Sp. were significantly lower and Tb.N. was significantly higher in the 15-day STS-131 samples compared to the 30-day Bion-M1 samples (Tb.Th: p=0.002, Tb.Sp.: p=0.014, Tb.N.: p=0.02). Notably, when comparing ground controls, Tb.Th. and Tb. Sp. were higher, and Tb.N. was lower, for STS-131 samples compared to Bion-M1 samples (Tb.Th.: p=0.002, Tb.Sp: p=0.10, Tb.N.: p=0.15).

Figure 3:

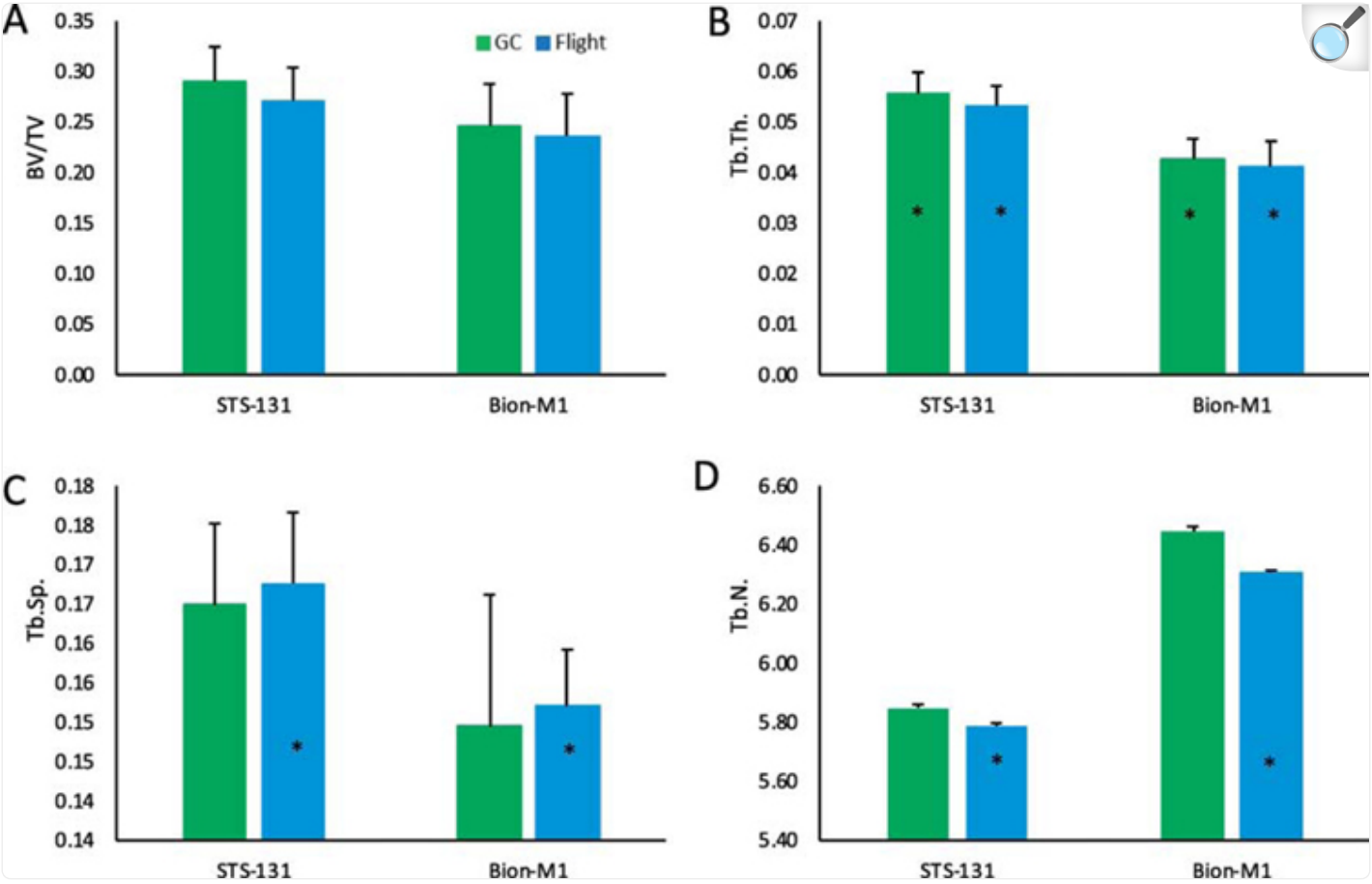

Open in a new tab

Spaceflight had no significant effect on the bone morphology of the humeral head. **(A)** bone volume over total volume (BV/TV), **(B)** trabecular thickness (Tb.Th.), **(C)** trabecular Spacing (Tb.S.), and **(D)** trabecular number (Tb.N.) were similar when comparing ground control to spaceflight samples. There were significant differences in most parameters when comparing STS-131 to Bion-M1 (i.e., GC STS-131 vs. GC Bion-M1 and flight STS-131 vs. flight Bion-M1, indicated by * within each bar).

When examining the bone morphometry of the calcaneus, no significant effects of spaceflight were seen in BV/TV (STS-131: p=0.31, STS-135: p=0.72, Bion-M1: p=0.91; Fig. S1). Cortical thickness was unchanged due to spaceflight, although there was a trend toward a decreased cortical thickness after the 15-day STS-131 mission (STS-131: p=0.08, STS-135: p=0.08, Bion-M1: p=0.77; Fig. S1). Trabecular structure was also unaffected by spaceflight (Tb.Th., STS-131: p=0.88, STS-135: p=0.43, Bion-M1: p=0.75; Tb.Sp., STS-131: p=0.81, STS-135: p=0.40, Bion-M1: p=0.67; Tb.N., STS-131: p=0.64, STS-135: p=0.33, Bion-M1: p=0.75; Fig. S1). When comparing the three missions, cortical

thickness, Tb.Sp. and Tb.Th. were decreased, and Tb.N. was increased, in the 30-day Bion-M1 mission compared to the shorter STS missions (Fig. S1). Notably, differences were also seen when comparing the ground controls among the three missions (Fig. S1).

3.4. Milliscale: Mechanical Properties

There were few changes to the mechanical properties of the supraspinatus tendon enthesis with spaceflight (Fig. 4). The structural properties maximum force and stiffness were not significantly different between spaceflight and ground controls for any of the missions (maximum force, STS-131: p=0.26, STS-135: p=0.33, Bion-M1: p=0.25; stiffness, STS-131: p=0.66, STS-135: p=0.52, Bion-M1: p=0.07). There were no significant differences in structural properties between the three missions. When examining material properties, maximum stress was not changed after 2 weeks of spaceflight (STS-131: p=0.18, STS-135: p=0.11), but there was a trend toward an increase after 4 weeks of spaceflight (Bion-M1: p=0.09). There was no significant difference in maximum stress between the three missions. Similarly, modulus was not changed after 2 weeks of spaceflight (STS-131: p=0.24, STS-135: p=0.11), but there was a significant increase after 4 weeks (Bion-M1: p=0.02). There was a significant difference in modulus when comparing STS-131 to STS-135. Resilience was not affected by spaceflight (STS-131: p=0.62, STS-135: p=0.43, Bion-M1: p=0.96). There were trends for decreased tendon cross-sectional area after 2 weeks of spaceflight (STS-131: p=0.08, STS-135: p=0.07, Fig. 4) and after 4 weeks of spaceflight (Bion-M1: p=0.05, Fig 4). There were no significant changes to failure area due to spaceflight (STS-131: p=0.49; Fig. 4).

There were few changes to the mechanical properties of the Achilles tendon enthesis with spaceflight (Fig. S2). Specifically, there were no significant changes to stiffness and modulus with spaceflight, although there was a trend towards an increased stiffness for the longer mission (stiffness, STS-135: p=0.73, Bion-M1: p=0.10; modulus, STS-135: p=0.37, Bion-M1: p=0.23). The cross-sectional area of the Achilles tendon increased with spaceflight after 2 weeks of spaceflight (STS-135: p=0.003) but was unchanged after 4 weeks of spaceflight (Bion-M1: p=0.69). There were no observable effects with mission on the cross-sectional area.

3.5. Gene expression

Gene expression data was collected for the humerus bone (Fig. 5A) and the rotator cuff tendon entheses (Figs. 5B, S3) from mice that flew on the 13 day STS-131 mission. For the humerus, expression of genes associated with mature osteoblasts (*Alp*, *Bsp*, *Col1*, *Osc*) were significantly upregulated in flight bones compared to ground control bones. Expression of genes associated with osteoblast differentiation were either unchanged (*Bmp2*, *Runx*) or decreased (*Osx*). Mechanoresponsiveness-associated genes showed decreased expression in some cases (*Cox2*, *Dkk1*) and increased expression in other cases (*Sost*) for flight bones compared to ground control bones. Expression of osteoclast-related genes (*CatK*, *Tnfsf11*) were significantly increased due to spaceflight. Expression of apoptosis promoters (*Bax, Casp*)

and inhibitors (*Bcl*) were significantly increased with spaceflight. Expression of adipogenesis promoters were increased in some cases (*Cebp*) and decreased in others (*Pparg2*) due to spaceflight. Expression of Wnt receptor-associated genes (*Lrp6, Postn, Sfrp*) were generally unchanged, with the exception of *Lrp5*, which was significantly increased with spaceflight. Expression of Wnt ligand-associated genes (*Wnt1, Wnt3a, Wnt10b*) were unchanged due to spaceflight.

Figure 5:

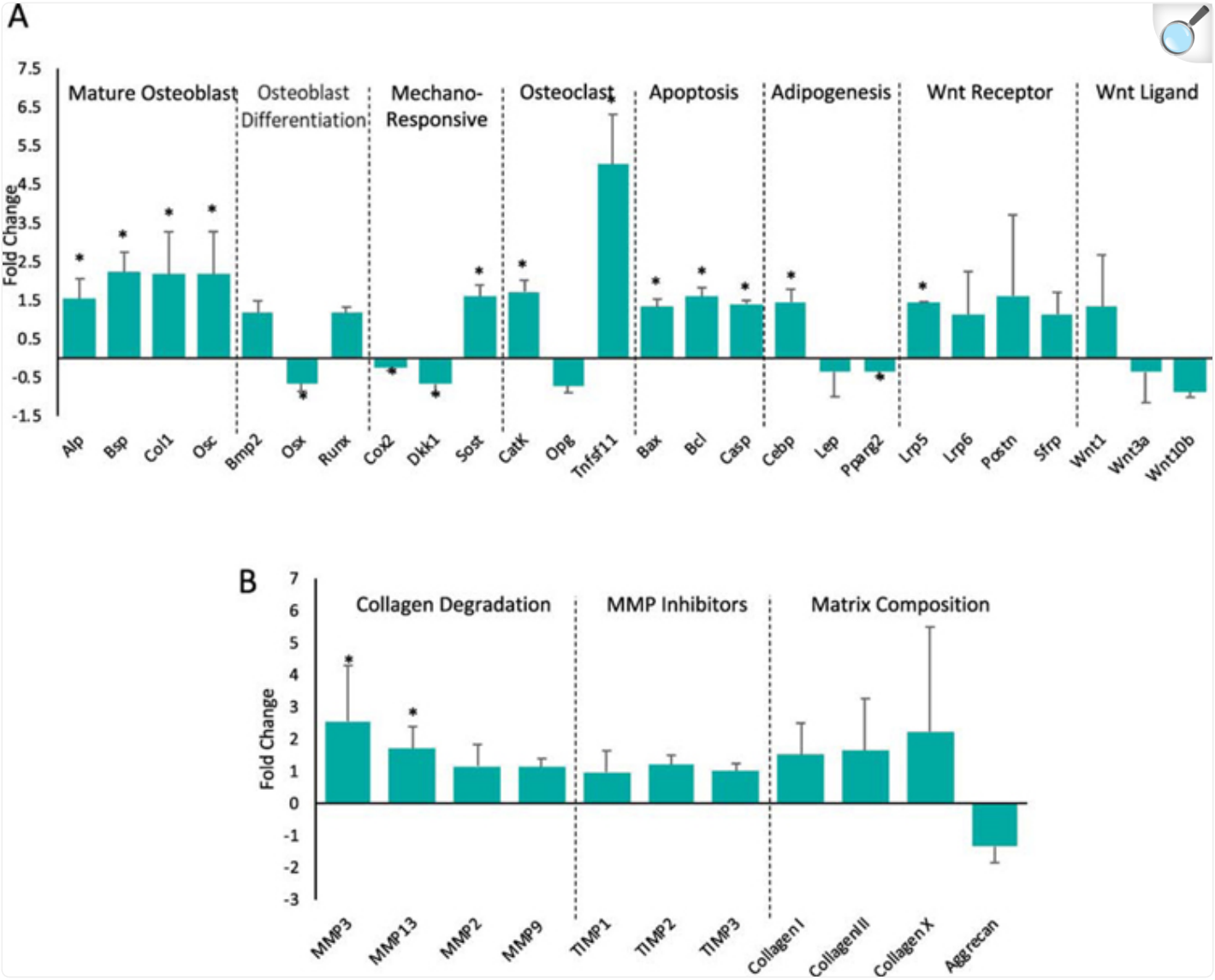

Open in a new tab

Fold change in gene expression of **(A)** humerus bones and **(B)** rotator cuff tendon entheses from spaceflight tissues relative to ground control tissues. (* indicates significant change, $p<0.05$, spaceflight compared to ground control).

Gene expression analysis of the supraspinatus tendon entheses demonstrated increased expression of extracellular matrix degradation-related genes due to spaceflight (Fig. 5B). Expression of matrix metalloproteinase genes *Mmp3* and *Mmp13* was increased in spaceflight entheses compared to ground control entheses. Other genes associated with

extracellular matrix remodeling (*Mmp2, Mmp9*, and Mmp inhibition-related *Timp1*, *Timp2*, *Timp3*) and extracellular matrix proteins (*Col1*, *Col3*, *Col10*, *Acan*) were unchanged with spaceflight. Gene expression analysis on the infraspinatus tendon entheses indicated no significant change with space flight (Fig. S3).

4. Discussion

Spaceflight led to significant changes to tendon and bone at the nanoscale (i.e., mineral carbonate levels and collagen fibril diameters) and to significant changes in gene expression in bone and enthesis tissues. However, these alterations did not lead to micro-and milliscale structural or mechanical changes in the tendon enthesis. These results demonstrate that the tendon enthesis is relatively robust to spaceflight conditions, although longer durations of spaceflight may result in structural and mechanical changes driven by the observed early nanoscale and gene expression effects.

In the current study, Achilles tendons from the Bion-M1 mission were examined via TEM to quantify the nanoscale collagen fibril structure. TEM images indicated that the average fibril size decreased with spaceflight. In addition, this decrease in fibril size represented not only a loss of larger fibrils, but a shift toward smaller fibrils across the entire tendon. Consistent with this, tendon enthesis cross-sectional area was decreased with spaceflight. Disuse as well as injury have been correlated to decreased tendon fibril size (19, 20). This decrease in fibril size may be the result of increased MMP activity in connective tissue of spaceflight mice; expression of collagen-degrading Mmps (*Mmp3, Mmp13*) was increased in the tendon entheses of spaceflight mice. This increase was not compensated for by Mmp inhibitors (*Timp1, Timp2, Timp3*), suggesting a possible net increase in matrix degradation during spaceflight. This has also been observed in earthbound unloaded murine Achilles tendons (21, 22). Despite this potentially Mmp-mediated decrease in collagen fibril diameter size, the mechanics of the tendon entheses were unaffected by spaceflight. Similarly, previous studies on the rotator cuff muscles of these mice indicated significant changes in gene expression but no changes in muscle structure due to spaceflight (18).

Raman analysis of the calcaneal bone showed that 15 days of spaceflight led to a decrease in bone mineral carbonate levels. This result is in agreement with the 7% decrease in carbonate content seen in the humeral heads of mice with paralyzed rotator cuffs (11) and the 2.6% decrease seen in hindlimb unloaded femurs (23). The level of carbonate content in bone changes due to bone aging, bone remodeling, and physio-chemical effects (24). Specifically, increased remodeling, which is commonly seen during unloading or spaceflight (25), has been shown to result in a decreased carbonate/phosphate peak ratio in murine femurs (26). In the current study, remodeling may also be responsible for the decrease in carbonate content, as spaceflight led to an increased expression of genes related to osteoclastogenesis (e.g., *CatK* and *Tnfsf11* [*Rankl*]), in agreement with previous studies (27). This increase in osteoclast markers was not mirrored by osteoblastogenesis gene expression, which showed either decreased (*Osx*) or did not change (*Bmp2, Runx*) with spaceflight, consistent with prior reports (28). In contrast, mature osteoblast activity, as indicated by expression of *Alp, Bsp, Col1*, and *Osc*, increased with spaceflight. Which together with the increased osteoclastogenic genes suggests increased bone remodeling. Such an increase in expression of mature ostoblast genes has not been previously reported

with unloading; osteoblast activity in unloaded conditions is usually limited by increased apoptosis and a shift towards adipose MSC differentiation (28–30). However, in the humeri studied here, spaceflight had contradictory effects on apoptosis- and adipogenesis-related genes. The ratio of *Bax/Bcl*, which is generally used as marker for apoptosis, was decreased with spaceflight, indicating increased survival. Yet, pro-apoptotic *Casp* was significantly increased. With adipogenesis, an increase in pro-adipogenesis *Cebp* gene expression was seen. However, there was also a decrease in adipocyte-associated *Pparg2*. These mixed adipogenesis and apoptosis results may point to a conflicting effect of spaceflight on osteoblasts. Nevertheless, gene expression results suggested increased bone resorption accompanied by increased bone formation. This increased remodeling may have led to the measured decrease in carbonate content, an indication of "younger" bone matrix (26). Although not apparent in the tendon enthesis mechanics of the current study, these changes in carbonate content can affect the size, structure, solubility, and mechanics of bone mineral crystals (31), leading to increased stiffness and decreased toughness (11).

The increase in osteoclastogenesis-associated genes in addition to the increase in bone formation genes suggests that there is increased remodeling or bone turnover but not necessarily an increase in bone resorption. The trabecular structure of the humeral head remained unchanged with both 2 and 4 weeks of spaceflight. This was unexpected, as microgravity is generally associated with bone loss. For the missions included in the current study, others reported decreases in BV/TV in the pelvis and mandibles of STS-131 animals (25, 32) as well as the vertebrae and femurs of the Bion-M1 animals (33, 34). Importantly, there is extensive evidence showing that bone loss with unloading varies dramatically with respect to anatomic site. For example, the femur, pelvis, and spine exhibit the highest levels of bone loss in unloading and spaceflight experiments (35, 36). Bones located at the extremities undergo less bone loss and sometimes even bone formation (36). For example, the BV/TV of the cranium and mandible increased in STS-131 and STS-135 respectively (37, 38). This effect is believed to result from fluid redistribution in microgravity increasing local pressure in the upper extremities (39). Furthermore, the rotator cuff acts as an active muscle stabilization system for the shoulder joint (40); this loading would persist in spaceflight conditions and could counteract any effects of microgravity.

There were significant differences in bone morphometry when comparing the 15 day STS-131 mission to the 30 day Bion-M1 mission, however, these differences were seen in both flight and ground control mice. Although the ages of the mice were similar between the two missions, the sex and breed of the mice were different (Table 1). Previous studies examining bone morphometry of C57BL/6J and C57BL/6N mice (i.e., the breeds of STS-131 and Bion-M1, respectively) showed no differences in Tb.Th. and Tb.Sp (41). The differences in the current study, therefore, were likely due to differences in sex. The Bion-M1 mice exhibit lower Tb.Th. and Tb.Sp. than the STS-131 mice, suggesting that these slightly older male mice may have had inherently thinner and more closely packed trabeculae than the younger female mice. This inference is contrary to data from most studies on sex effects, which show that females have thinner trabeculae with more space (42); however, the differences observed here may be the result of combined age, gender, and breed effects.

Despite significant changes to the nanoscale structures of the tendon entheses, no changes were observed due to

spaceflight in the mechanics of the supraspinatus and Achilles tendon entheses. Even with measurable decreases in the tendon cross-sectional area (in agreement with (43)), the stiffness and maximum force of the entheses were unaffected, suggesting that the rotator cuff and Achilles tendon-to-bone attachments were able to carry matching loads before and after 2 or 4 weeks of spaceflight. Although this result is in agreement with unloading studies that showed no changes in stiffness of the tendon enthesis after 3 weeks of unloading (11), it goes against the more accepted view that unloading and spaceflight lead to decreases in bone and tendon stiffness (3). The results demonstrate that the attachment of tendon to bone is not sensitive to short durations of spaceflight; loss of tendon mass and changes to bone mineralization did not affect the load-carrying capacity of the enthesis. To determine material properties, maximum force and stiffness were normalized to the tissue geometry (i.e., tendon length and cross-sectional area). This resulted in increased maximum stress and modulus in Bion-M1 spaceflight mice compared to ground control mice. These increases in material properties were unexpected, as both tendon and bone moduli have generally been shown to decrease with unloading (3, 34). However, some studies have reported increases in tendon modulus with unloading (44). The increased material properties coupled with the decreased tendon cross-sectional area indicates that the mechanics of the tendon enthesis are not driven by the bulk tissue geometry, and that the attachment is robust to changes in the tendon and bone.

5. Conclusions

Spaceflight had significant effects on bone composition, tendon microstructure, and gene expression. Fifteen days of spaceflight was sufficient to cause a decrease in the carbonate content of calcaneal bone that could lead to changes in bone nanostructure and mechanics. This compositional change was likely the result of increased remodeling, as evidenced by increases in osteoclastogenesis- and mature osteoblast activity-related genes. Similarly, Achilles tendons exhibited a shift in tendon collagen fibril size towards smaller diameters. Increased catabolic activity may have led to this decrease in fibril size, as Mmp3 and 13 expression were increased. Despite these nanoscale structure and gene expression changes, spaceflight had little effect on the morphology and mechanics of the tendon enthesis, implying that the attachment may be insensitive to short durations of spaceflight.

Supplementary Material

1

NIHMS1544144-supplement-1.pdf (46.9KB, pdf)

2

NIHMS1544144-supplement-2.pdf (44.6KB, pdf)

3

NIHMS1544144-supplement-3.pdf (31.5KB, pdf)

Highlights:

- The supraspinatus tendon entheses of mice was compositionally, genetically, structurally and mechanically characterized after 2–4 weeks of spaceflight.
- Space flight led to a decrease in carbonate levels in the mineralized tissue, likely due to increased bone remodeling.
- Increased expression of collagen degradation-associated genes caused decreased Achilles tendon fibril size with spaceflight.
- Enthesis microstructure and mechanics was unchanged with spaceflight, suggesting a resistance to degradation during short-term microgravity.

Acknowledgments

This project was funded by the National Aeronautics and Space Administration (NASA, NNX09AP05G to ST), the National Space Biomedical Research Institute (NSBRI, NSBRI-RFA-13–01 to ACD), and the National Institutes of Health (NIH R01-AR055580 to ST; NIH R01 AR047867 to MJS). The TEM studies were partially supported by the Institute of Materials Science & Engineering at Washington University. The authors thank Ashley Williams for help collecting microCT data. We thank Jill Pasteris for assistance in collection and analysis of the Raman data.

Abbreviations:

CA

calcaneus-Achilles tendon complex

HS

Humerus-Supraspinatus tendon complex

FL

Space Flight

GC

Ground Control

Footnotes

References

1. Martin TP, Edgerton VR, and Grindeland RE. (1988) Influence of Spaceflight on Rat Skeletal Muscle. J. Appl. Physiol 65, 2318–2325 [DOI] [PubMed] [Google Scholar]

2. Fitts RH, Riley DR, and Widrick JJ. (2000) Physiology of a Microgravity Environment Invited Review: Microgravity and Skeletal Muscle. J. Appl. Physiol 89, 823–839 [DOI] [PubMed] [Google Scholar]

3. Narici MV, and Boer MD. (2011) Disuse of the Musculo-Skeletal System in Space and on Earth. Eur J Appl Physiol 111, 403–420 [DOI] [PubMed] [Google Scholar]

4. Nagaraja MP, and Risin D. (2013) The Current State of Bone Loss Research: Data from Spaceflight and Microgravity Simulators. Journal of cellular biochemistry 114, 1001–1008 [DOI] [PubMed] [Google Scholar]

5. Comte T, Lau A, Livingston E, Ellman R, Spatz J, Stodieck L, Bouxsein M, Ferguson V, and Bateman T. (2014) Comparing Proximal Tibia Bone Stiffness and Structural Efficiency in Spaceflight and Hind Limb Unloading with a Sclerostin Antibody Counter-Measure In JOURNAL OF BONE AND MINERAL RESEARCH Vol. 29 pp. S134–S134, WILEY-BLACKWELL 111 RIVER ST, HOBOKEN 07030–5774, NJ USA [Google Scholar]

6. Cann CE. (1993) Adaptations of the Skeletal System to Spaceflight In Introduction to Space Life Science (Churchill S, ed) [Google Scholar]

7. Saadat F, Deymier AC, Birman V, Thomopoulos S, and Genin GM. (2016) The Concentration of Stress at the Rotator Cuff Tendon-to-Bone Attachment Site Is Conserved across Species. J. Mech. Behav. Biomed. Mater 62, 24–32 [DOI] [PMC free article] [PubMed] [Google Scholar]

8. Thomopoulos S, Marquez JP, Weinberger B, Birman V, and Genin GM. (2006) Collagen Fiber Orientation at the Tendon to Bone Insertion and Its Influence on Stress Concentrations. J. Biomech 39, 1842–1851 [DOI] [PubMed] [Google Scholar]

9. Genin GM, Kent A, Birman V, Wopenka B, Pasteris JD, Marquez PJ, and Thomopoulos S. (2009) Functional Grading of Mineral and Collagen in the Attachment of Tendon to Bone. Biophys J 97, 976–985 [DOI] [PMC free article] [PubMed] [Google Scholar]

10. Tempelhof S, Rupp S, and Seil R. (1999) Age-Related Prevalence of Rotator Cuff Tears in Asymptomatic Shoulders. J Shoulder Elbow Surg 8, 296–299 [DOI] [PubMed] [Google Scholar]

11. Deymier AC, Schwartz AG, Cai Z, Daulton TL, Pasteris JD, Genin GM, and Thomopoulos S. (2019) The Multiscale Structural and Mechanical Effects of Mouse Supraspinatus Muscle Unloading on the Mature Enthesis. Acta Biomater 83, 302–313 [DOI] [PMC free article] [PubMed] [Google Scholar]

12. Andreev-Andrievskiy A, Popova A, Boyle R, Alberts J, Shenkman B, Vinogradova O, Dolgov O, Anokhin K, Tsvirkun D, Soldatov P, Nemirovskaya T, Ilyin E, and Sychev V. (2014) Mice in Bion-M 1 Space Mission: Training and Selection. PLOS ONE 9, e104830. [DOI] [PMC free article] [PubMed] [Google Scholar]

13. Ulanova A, Gritsyna Y, Vikhlyantsev I, Salmov N, Bobylev A, Abdusalamova Z, Rogachevsky V, Shenkman B, and Podlubnaya Z. (2015) Isoform Composition and Gene Expression of Thick and Thin Filament Proteins in Striated Muscles of Mice after 30-Day Space Flight. BioMed Research International 2015, 13. [DOI] [PMC free article] [PubMed] [Google Scholar]

14. Wopenka B, Kent A, Pasteris JD, Yoon Y, and Thomopoulos S. (2008) The Tendon-to-Bone Transition of the Rotator Cuff: A Preliminary Raman Spectroscopic Study Documenting the Gradual Mineralization across the Insertion in Rat Tissue Samples. Applied spectroscopy 62, 1285–1294 [DOI] [PMC free article] [PubMed] [Google Scholar]

15. Schwartz AG, Pasteris JD, Genin GM, Daulton TL, and Thomopoulos S. (2012) Mineral Distributions at the Developing Tendon Enthesis. PLoS One 7, 9. [DOI] [PMC free article] [PubMed] [Google Scholar]

16. Schwartz AG, Lipner JH, Pasteris JD, Genin GM, and Thomopoulos S. (2013) Muscle Loading Is

Necessary for the Formation of a Functional Tendon Enthesis. Bone 55, 44–51 [DOI] [PMC free article] [PubMed] [Google Scholar]

17. Rasband W. (1997–2009) Imagej U. S. National Institutes of Health, Bethesda, MA [Google Scholar]

18. Shen H, Lim C, Schwartz AG, Andreev-Andrievskiy A, Deymier AC, and Thomopoulos S. (2017) Effects of Spaceflight on the Muscles of the Murine Shoulder. The FASEB Journal 31, 5466–5477 [DOI] [PMC free article] [PubMed] [Google Scholar]

19. Nakagawa Y, Totsuka M, Sato T, Fukuda Y, and Hirota K. (1989) Effect of Disuse on the Ultrastructure of the Achilles Tendon in Rats. European journal of applied physiology and occupational physiology 59, 239–242 [DOI] [PubMed] [Google Scholar]

20. Reeves ND, Narici MV, and Maganaris CN. (2006) Myotendinous Plasticity to Ageing and Resistance Exercise in Humans. Experimental physiology 91, 483–498 [DOI] [PubMed] [Google Scholar]

21. Mori N, Majima T, Iwasaki N, Kon S, Miyakawa K, Kimura C, Tanaka K, Denhardt DT, Rittling S, Minami A, and Uede T. (2007) The Role of Osteopontin in Tendon Tissue Remodeling after Denervation-Induced Mechanical Stress Deprivation. Matrix Biology 26, 42–53 [DOI] [PubMed] [Google Scholar]

22. Leigh DR, Abreu EL, and Derwin KA. (2008) Changes in Gene Expression of Individual Matrix Metalloproteinases Differ in Response to Mechanical Unloading of Tendon Fascicles in Explant Culture. J. Orthopaed. Res 26, 1306–1312 [DOI] [PMC free article] [PubMed] [Google Scholar]

23. Mandair S, G., Bateman T, and Morris D, M (2009) Raman Spectroscopy of Murine Bone in Response to Simulated Spaceflight Conditions Vol. 7166 [Google Scholar]

24. Boskey AL, and Imbert L. (2017) Bone Quality Changes Associated with Aging and Disease: A Review. Ann N Y Acad Sci 1410, 93–106 [DOI] [PMC free article] [PubMed] [Google Scholar]

25. Blaber EA, Dvorochkin N, Lee C, Alwood JS, Yousuf R, Pianetta P, Globus RK, Burns BP, and Almeida E. a. C. (2013) Microgravity Induces Pelvic Bone Loss through Osteoclastic Activity, Osteocytic Osteolysis, and Osteoblastic Cell Cycle Inhibition by Cdkn1a/P21. PLOS ONE 8, e61372. [DOI] [PMC free article] [PubMed] [Google Scholar]

26. Isaksson H, Turunen MJ, Rieppo L, Saarakkala S, Tamminen IS, Rieppo J, Kroger H, and Jurvelin JS. (2010) Infrared Spectroscopy Indicates Altered Bone Turnover and Remodeling Activity in Renal Osteodystrophy. J Bone Miner Res 25, 1360–1366 [DOI] [PubMed] [Google Scholar]

27. Tamma R, Colaianni G, Camerino C, Di Benedetto A, Greco G, Strippoli M, Vergari R, Grano A, Mancini L, Mori G, Colucci S, Grano M, and Zallone A. (2009) Microgravity During Spaceflight Directly Affects in

Vitro Osteoclastogenesis and Bone Resorption. FASEB journal : official publication of the Federation of American Societies for Experimental Biology 23, 2549–2554 [DOI] [PubMed] [Google Scholar]

28. Zhang C, Li L, Jiang Y, Wang C, Geng B, Wang Y, Chen J, Liu F, Qiu P, Zhai G, Chen P, Quan R, and Wang J. (2018) Space Microgravity Drives Transdifferentiation of Human Bone Marrow–Derived Mesenchymal Stem Cells from Osteogenesis to Adipogenesis. The FASEB Journal 32, 4444–4458 [DOI] [PubMed] [Google Scholar]

29. Nakamura H, Kumei Y, Morita S, Shimokawa H, Ohya K, and Shinomiya K. (2003) Suppression of Osteoblastic Phenotypes and Modulation of Pro- and Anti-Apoptotic Features in Normal Human Osteoblastic Cells under a Vector-Averaged Gravity Condition. Journal of medical and dental sciences 50, 167–176 [PubMed] [Google Scholar]

30. Nakamura H, Kumei Y, Morita S, Shimokawa H, Ohya K, and Shinomiya K. (2003) Antagonism between Apoptotic (Bax/Bcl-2) and Anti-Apoptotic (Iap) Signals in Human Osteoblastic Cells under Vector-Averaged Gravity Condition. Ann. N.Y. Acad. Sci 1010, 143–147 [DOI] [PubMed] [Google Scholar]

31. Deymier AC, Nair AK, Depalle B, Qin Z, Arcot K, Drouet C, Yoder CH, Buehler MJ, Thomopoulos S, Genin GM, and Pasteris JD. (2017) Protein-Free Formation of Bone-Like Apatite: New Insights into the Key Role of Carbonation. Biomaterials 127, 75–88 [DOI] [PMC free article] [PubMed] [Google Scholar]

32. Ghosh P, Stabley JN, Behnke BJ, Allen MR, and Delp MD. (2016) Effects of Spaceflight on the Murine Mandible: Possible Factors Mediating Skeletal Changes in Non-Weight Bearing Bones of the Head. Bone 83, 156–161 [DOI] [PubMed] [Google Scholar]

33. Berg-Johansen B, Liebenberg EC, Li A, Macias BR, Hargens AR, and Lotz JC. (2016) Spaceflight-Induced Bone Loss Alters Failure Mode and Reduces Bending Strength in Murine Spinal Segments. J Orthop Res 34, 48–57 [DOI] [PMC free article] [PubMed] [Google Scholar]

34. Gerbaix M, Gnyubkin V, Farlay D, Olivier C, Ammann P, Courbon G, Laroche N, Genthial R, Follet H, Peyrin F, Shenkman B, Gauquelin-Koch G, and Vico L. (2017) One-Month Spaceflight Compromises the Bone Microstructure, Tissue-Level Mechanical Properties, Osteocyte Survival and Lacunae Volume in Mature Mice Skeletons. Scientific reports 7, 2659. [DOI] [PMC free article] [PubMed] [Google Scholar]

35. Leblanc A, Schneider V, Shackelford L, West S, Oganov V, Bakulin A, and Voronin L. (2000) Bone Mineral and Lean Tissue Loss after Long Duration Space Flight. J Musculoskelet Neuronal Interact 1, 157–160 [PubMed] [Google Scholar]

36. Mccarthy I, Goodship A, Herzog R, Oganov V, Stussi E, and Vahlensieck M. (2000) Investigation of Bone Changes in Microgravity During Long and Short Duration Space Flight: Comparison of Techniques. European Journal of Clinical Investigation 30, 1044–1054 [DOI] [PubMed] [Google Scholar]

37. Zhang B, Cory E, Bhattacharya R, Sah R, and Hargens AR. (2013) Fifteen Days of Microgravity Causes Growth in Calvaria of Mice. Bone 56, 290–295 [DOI] [PMC free article] [PubMed] [Google Scholar]

38. Dagdeviren D, Kalajzic Z, Adams DJ, Kalajzic I, Lurie A, Mednieks MI, and Hand AR. (2018) Responses to Spaceflight of Mouse Mandibular Bone and Teeth. Arch Oral Biol 93, 163–176 [DOI] [PubMed] [Google Scholar]

39. Mccarthy ID. (2005) Fluid Shifts Due to Microgravity and Their Effects on Bone: A Review of Current Knowledge. Annals of Biomedical Engineering 33, 95–103 [DOI] [PubMed] [Google Scholar]

40. O'brien MJ, and Savoie FH. (2018) 22 - Rotator Cuff Tendinitis in the Overhead Athlete In Clinical Orthopaedic Rehabilitation: A Team Approach (Fourth Edition) (Giangarra CE, and Manske RC, eds) pp. 110–116.e111, Content Repository Only!, Philadelphia [Google Scholar]

41. Simon MM, Greenaway S, White JK, Fuchs H, Gailus-Durner V, Wells S, Sorg T, Wong K, Bedu E, Cartwright EJ, Dacquin R, Djebali S, Estabel J, Graw J, Ingham NJ, Jackson IJ, Lengeling A, Mandillo S, Marvel J, Meziane H, Preitner F, Puk O, Roux M, Adams DJ, Atkins S, Ayadi A, Becker L, Blake A, Brooker D, Cater H, Champy M-F, Combe R, Danecek P, Di Fenza A, Gates H, Gerdin A-K, Golini E, Hancock JM, Hans W, Hölter SM, Hough T, Jurdic P, Keane TM, Morgan H, Müller W, Neff F, Nicholson G, Pasche B, Roberson L-A, Rozman J, Sanderson M, Santos L, Selloum M, Shannon C, Southwell A, Tocchini-Valentini GP, Vancollie VE, Westerberg H, Wurst W, Zi M, Yalcin B, Ramirez-Solis R, Steel KP, Mallon A-M, De Angelis MH, Herault Y, and Brown SD. (2013) A Comparative Phenotypic and Genomic Analysis of C57bl/6j and C57bl/6n Mouse Strains. Genome Biology 14, R82. [DOI] [PMC free article] [PubMed] [Google Scholar]

42. Florian B, Matthias G, Timo BF, Eik V, Marcus M, Martin R, Pia P, Karl W, M., R. J., Klaus P, and Michael A. (2010) Age- and Sex-Related Changes of Humeral Head Microarchitecture: Histomorphometric Analysis of 60 Human Specimens. J. Orthopaed. Res 28, 18–26 [DOI] [PubMed] [Google Scholar]

43. B., J. R., K., T. A., R., J. K., A., B. R., A., T. M., and A., B. H (2005) Effects of Spaceflight on the Attachment of Tendons to Bone in the Hindlimb of the Pregnant Rat. The Anatomical Record Part A: Discoveries in Molecular, Cellular, and Evolutionary Biology 282A, 147–156 [DOI] [PubMed] [Google Scholar]

44. Khayyeri H, Blomgran P, Hammerman M, Turunen MJ, Löwgren A, Guizar-Sicairos M, Aspenberg P, and Isaksson H. (2017) Achilles Tendon Compositional and Structural Properties Are Altered after Unloading by Botox. Scientific reports 7, 13067. [DOI] [PMC free article] [PubMed] [Google Scholar]

Associated Data

This section collects any data citations, data availability statements, or supplementary materials included in this article.

Supplementary Materials

1

NIHMS1544144-supplement-1.pdf (46.9KB, pdf)

2

NIHMS1544144-supplement-2.pdf (44.6KB, pdf)

3

NIHMS1544144-supplement-3.pdf (31.5KB, pdf)